

## THERMAL STABILITY OF SOME FERROCENE CONTAINING SCHIFF BASES

Irina Cărlescu, Gabriela Lisa \* and D. Scutaru

\*Gh. Asachi' Technical University Iasi, Faculty of Chemical Engineering, Bd. D. Mangeron, No. 71, 700050 Iasi, Romania

Taking into account the importance of thermal stability in the liquid crystals field, the study presents the thermal behavior of some ferrocene containing Schiff bases. Some other kinetic characteristics, such as reaction order ( $n$ ), activation energy ( $E_a$ ) and pre-exponential factor ( $\ln A$ ) have been also evaluated. The thermal stability series of Schiff bases was established analysis associated with three parameters ( $T_d$ ,  $T_{max}$ ,  $E_a$ ) is:  $S_6 < S_4 < S_3 < S_5 < S_1 < S_2$ .

**Keywords:** ferrocene containing Schiff bases, kinetic characteristics, thermal degradation

### Introduction

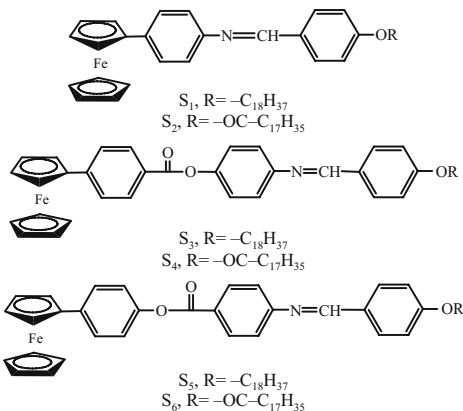
Liquid crystal phases are often referred to as a fourth state of matter. Various applications based on liquid crystal phases are of importance in every day life. They are indispensable in biological systems (e.g. membranes) and are becoming an increasing part of high-tech processes.

Although thermal stability of polymeric liquid crystals has been extensively studied [1–4], only a minor attention has been paid to the small molecular liquid crystals [5–10].

Liquid crystalline materials containing ferrocene are attracting special attention because of the ability of the transition metal center to impart unique optical, magnetic and electrical properties [11]. More than that, ferrocene exhibits the properties of a typical aromatic molecule and is stable to more than 500°C. The presence of the ferrocene into liquid crystalline compounds induces a monotropic or enantiotropic behavior [12].

Thermal stability represents an important parameter that may affect the use of new compounds, especially into domains that require treatment at elevated temperatures [9, 10]. In the case of liquid crystals, alongside to the especially properties: fluidity, optical birefringence, compounds must be thermally stable in the temperature range of the mesophase domain.

The paper presents the study of the thermal stability of some ferrocene derivatives presented in Scheme 1. Ferrocene derivatives  $S_3$ – $S_6$  presented broad enantiotropic liquid crystalline phases. The degradation process is complex and depends on the mesogenic units attached to the ferrocene.



**Scheme 1** The chemical structure of the target compounds

### Experimental

#### Materials

Silica gel 60 (Merck) was used for column chromatography. TLC was performed on Silicagel F<sub>254</sub> plates (Merck). The used amino and aldehydic compounds were previously prepared in our laboratory.

#### General procedure for sample preparation

To a stirred solution containing the amino and aldehydic compounds in ethanol a few drops of glacial acetic acid were added. The solution was refluxed with stirring for 6 h. The mixture was filtered while hot and the solid was washed on filter with hot ethanol. The resulting solid was recrystallised from ethanol or purified by column chromatography (CC).

\* Author for correspondence: gapreot@ch.tuiasi.ro

**4-Octadecyloxybenzylidene-4-ferrocenylphenylamine (S<sub>1</sub>)**

Quantities: 0.3 g (1.08 mmol) 4-ferrocenylaniline in 30 mL ethanol, 0.405 g (1.08 mmol) 4-octadecyloxybenzaldehyde, glacial acetic acid (catalytic). The product was recrystallised from ethanol. Yield: 74.4% (0.51 g), *m.p.*: 109–112°C. IR (KBr, cm<sup>-1</sup>): 2918, 2848, 1606, 1570, 1516, 1469, 1309, 1247, 1168, 1029, 842. <sup>1</sup>H-NMR δ<sub>H</sub> (CDCl<sub>3</sub>): 8.38 (s, 1H, CH), 7.78 (d, 2H, ArH), 7.43 (d, 2H, ArH), 7.09 (d, 2H, ArH), 6.91 (d, 2H, ArH), 4.58 (t, 2H, C<sub>5</sub>H<sub>4</sub>), 4.25 (t, 2H, C<sub>5</sub>H<sub>4</sub>), 3.98 (s, 5H, C<sub>5</sub>H<sub>5</sub>), 3.95 (t, 2H, -OCH<sub>2</sub>-), 1.74 (m, 2H, -CH<sub>2</sub>-), 1.40–1.19 (m, 30H, 15CH<sub>2</sub>), 0.81 (t, 3H, -CH<sub>3</sub>). *m/z*: 631 [M-2]<sup>+</sup>.

**4-(4-Ferrocenylphenyliminomethyl)benzoic acid heptadecyl ester (S<sub>2</sub>)**

Quantities: 0.25 g (0.90 mmol) 4-ferrocenylaniline in 30 mL ethanol, 0.35 g (0.90 mmol) 4-octadecyloxybenzaldehyde, glacial acetic acid (catalytic). The product was recrystallised from ethanol. Yield: 46% (0.269 g), *m.p.*: 115°C. IR (KBr, cm<sup>-1</sup>): 2914, 2848, 1751, 1685, 1656, 1598, 1465, 1384, 1219, 1157, 925, 840. <sup>1</sup>H-NMR δ<sub>H</sub> (CDCl<sub>3</sub>): 8.49 (s, 1H, CH), 7.92 (d, 2H, ArH), 7.49 (d, 2H, ArH), 7.18 (m, 4H, ArH), 4.64 (t, 2H, C<sub>5</sub>H<sub>4</sub>), 4.31 (t, 2H, C<sub>5</sub>H<sub>4</sub>), 4.03 (s, 5H, C<sub>5</sub>H<sub>5</sub>), 2.56 (t, 2H, -OC-CH<sub>2</sub>-), 1.75 (m, 2H, -CH<sub>2</sub>-), 1.57–1.24 (m, 28H, 14CH<sub>2</sub>), 0.86 (t, 3H, -CH<sub>3</sub>). *m/z*: 645 [M-2]<sup>+</sup>.

**4-Ferrocenylbenzoic acid 4-[(4-octadecyloxybenzylidene)amino]phenyl ester (S<sub>3</sub>)**

Quantities: 0.3 g (0.755 mmol) 4-aminophenyl-4-ferrocenylbenzoate in 30 mL ethanol, 0.282 g (0.755 mmol) 4-octadecyloxybenzaldehyde, glacial acetic acid (1–2 drops). Purification: CC/silica gel/CH<sub>2</sub>Cl<sub>2</sub>: petroleum ether: TEA=1:4:3%, Yield: 43.9% (0.25 g), *m.p.* (liquid crystal): 79°C (K<sub>1</sub>/K<sub>2</sub>), 133°C (K<sub>2</sub>/CL), 144°C (CL/I), 143°C (I/CL), 118°C (CL/K<sub>2</sub>), 34°C (K<sub>2</sub>/K<sub>1</sub>). IR (KBr, cm<sup>-1</sup>): 2918, 2848, 1726 (>C=O), 1604, 1570, 1508, 1255, 1180, 813. <sup>1</sup>H-NMR δ<sub>H</sub> (CDCl<sub>3</sub>): 8.41 (s, 1H, CH), 8.13 (d, 2H, ArH), 7.85 (d, 2H, ArH), 7.59 (d, 2H, ArH), 7.25 (m, 4H, ArH), 6.99 (d, 2H, ArH), 4.75 (t, 2H, C<sub>5</sub>H<sub>4</sub>), 4.42 (t, 2H, C<sub>5</sub>H<sub>4</sub>), 4.06 (s, 5H, C<sub>5</sub>H<sub>5</sub>), 4.02 (t, 2H, -O-CH<sub>2</sub>-), 1.79 (m, 2H, -CH<sub>2</sub>-), 1.51–1.26 (m, 30H, 15CH<sub>2</sub>), 0.88 (t, 3H, -CH<sub>3</sub>). <sup>13</sup>C-NMR δ<sub>C</sub> (CDCl<sub>3</sub>): 163.2 (>C=O), 159.9 (-CH=N-), 157.8, 147.9, 146.7, 144.0, 128.4, 128.2, 126.8, 124.7, 123.7, 120.26, 119.7, 112.6, (12 C aromatic), 81.3, 67.9, 67.8, 66.2, 64.9 (5 C, C<sub>5</sub>H<sub>5</sub>, C<sub>5</sub>H<sub>4</sub> and -O-CH<sub>2</sub>-), 29.8, -12.0 (17 C, aliphatic). *m/z*: 752 [M-1]<sup>+</sup>.

**4-Ferrocenylbenzoic acid 4-[(4-octadecanoyloxybenzylidene)amino]phenyl ester (S<sub>4</sub>)**

Quantities: 0.35 g (0.881 mmol) 4-aminophenyl-4-ferrocenylbenzoate in 30 mL ethanol, 0.342 g (0.881 mmol) 4-octadecanoyloxybenzaldehyde, glacial acetic acid (1–2 drops). Purification: CC/silica gel/CH<sub>2</sub>Cl<sub>2</sub>: petroleum ether: TEA=1:4:3%. Yield: 53.2% (0.36 g), *m.p.* (liquid crystal): 114°C (K<sub>1</sub>/K<sub>2</sub>), 126°C (K<sub>2</sub>/CL), 153°C (CL/I), 151°C (I/CL), 104°C (CL/K<sub>2</sub>), 82°C (K<sub>2</sub>/K<sub>1</sub>). IR (KBr, cm<sup>-1</sup>): 2920, 2848, 1761, 1724, 1602, 1504, 1265, 1178, 815. <sup>1</sup>H-NMR δ<sub>H</sub> (CDCl<sub>3</sub>): 8.47 (s, 1H, CH), 8.13 (d, 2H, ArH), 7.95 (d, 2H, ArH), 7.59 (d, 2H, ArH), 7.26 (m, 4H, ArH), 7.22 (d, 2H, ArH), 4.75 (t, 2H, C<sub>5</sub>H<sub>4</sub>), 4.43 (t, 2H, C<sub>5</sub>H<sub>4</sub>), 4.06 (s, 5H, C<sub>5</sub>H<sub>5</sub>), 2.58 (t, 2H, -OC-CH<sub>2</sub>-), 1.77 (m, 2H, -CH<sub>2</sub>-), 1.43–1.26 (m, 28H, 14CH<sub>2</sub>), 0.88 (t, 2H, -CH<sub>3</sub>). <sup>13</sup>C-NMR δ<sub>C</sub> (CDCl<sub>3</sub>): 172.3 (>C=O), 165.7 (>C=O), 159.6 (-CH=N-), 153.6, 149.9, 149.6, 146.5, 134.1, 130.1, 130.4, 126.9, 126.1, 122.8, 122.5, 122.2 (12 C aromatic), 83.4, 70.4, 70.3, 67.4 (4 C, C<sub>5</sub>H<sub>4</sub> and C<sub>5</sub>H<sub>5</sub>), 34.8–14.5 (17 C aliphatic). *m/z*: 766 [M-1]<sup>+</sup>.

**4-[(4-Octadecyloxybenzylidene)amino]benzoic acid 4-ferrocenylphenyl ester (S<sub>5</sub>)**

Quantities: 0.2 g (0.503 mmol) 4-ferrocenylphenyl-4-aminobenzoate in 20 mL ethanol, 0.188 g (0.503 mmol) 4-octadecyloxybenzaldehyde, glacial acetic acid (1–2 drops). Purification: CC/silica gel/CH<sub>2</sub>Cl<sub>2</sub>: petroleum ether: TEA=1:4:3%. Yield: 63% (0.425 g), *m.p.* (liquid crystal): 97°C (K<sub>1</sub>/K<sub>2</sub>), 114°C (K<sub>2</sub>/CL), 145°C (CL/I), 143°C (I/CL), 76°C (CL/K<sub>2</sub>), 32°C (K<sub>2</sub>/K<sub>1</sub>). IR (KBr, cm<sup>-1</sup>): 2918, 2848, 1753, 1593, 1571, 1251, 1165, 812. <sup>1</sup>H-NMR δ<sub>H</sub> (CDCl<sub>3</sub>): 8.43 (s, 1H, CH), 8.25 (d, 2H, ArH), 7.87 (d, 2H, ArH), 7.49 (d, 2H, ArH), 7.26 (m, 4H, ArH), 7.13 (d, 2H, ArH), 4.72 (t, 2H, C<sub>5</sub>H<sub>4</sub>), 4.39 (t, 2H, C<sub>5</sub>H<sub>4</sub>), 4.14 (s, 5H, C<sub>5</sub>H<sub>5</sub>), 4.03 (t, 2H, -O-CH<sub>2</sub>-), 1.79 (m, 2H, -CH<sub>2</sub>-), 1.44–1.26 (m, 30H, 15CH<sub>2</sub>), 0.88 (t, 2H, -CH<sub>3</sub>). <sup>13</sup>C-NMR δ<sub>C</sub> (CDCl<sub>3</sub>): 163.05 (>C=O), 160.05 (-CH=N-), 156.8, 153.7, 148.28, 137.1, 133.4, 131.6, 128.4, 125.2, 124.8, 121.5, 118.6, 120.6 (12 C aromatic), 69.8, 67.9, 67.3, 66.7, 65.0 (C<sub>5</sub>H<sub>4</sub>, C<sub>5</sub>H<sub>5</sub> and -OCH<sub>2</sub>), 29.5–11.7 (17 C, aliphatic). *m/z*: 752 [M-1]<sup>+</sup>.

**4-[(4-Octadecanoyloxybenzylidene)amino]benzoic acid 4-ferrocenylphenyl ester (S<sub>6</sub>)**

Quantities: 0.35 g (0.88 mmol) 4-ferrocenylphenyl-4-aminobenzoate in 25 mL ethanol, 0.342 g (0.88 mmol) 4-octadecanoyloxybenzaldehyde, glacial acetic acid (1–2 drops). Purification: CC/silica gel/CH<sub>2</sub>Cl<sub>2</sub>: petroleum ether: TEA=1:4:3%. Yield: 63% (0.425 g), *m.p.* (liquid crystal): 66°C (K<sub>1</sub>/K<sub>2</sub>), 129°C (K<sub>2</sub>/CL), 155°C (CL/I), 151°C (I/CL), 67°C (CL/K<sub>2</sub>),

55°C ( $K_2/K_1$ ). IR (KBr,  $\text{cm}^{-1}$ ): 2918, 2848, 1751, 1723, 1627, 1595, 1278, 1211, 1161, 825.  $^1\text{H-NMR}$   $\delta_{\text{H}}$  ( $\text{CDCl}_3$ ): 8.45 (s, 1H,  $-\text{CH}-$ ), 8.25 (d, 2H, ArH), 7.97 (d, 2H, ArH), 7.49 (d, 2H, ArH), 7.28 (m, 2H, ArH), 7.25 (d, 2H, ArH), 7.16 (d, 2H, ArH), 4.72 (t, 2H,  $\text{C}_5\text{H}_4$ ), 4.40 (t, 2H,  $\text{C}_5\text{H}_4$ ), 4.14 (s, 5H,  $\text{C}_5\text{H}_5$ ), 2.59 (t, 2H,  $-\text{O}-\text{CO}-\text{CH}_2-$ ), 1.77 (m, 2H,  $-\text{CH}_2-$ ), 1.43–1.26 (m, 28H, 14 $\text{CH}_2$ ), 0.88 (t, 3H,  $-\text{CH}_3$ ).  $^{13}\text{C-NMR}$   $\delta_{\text{C}}$  ( $\text{CDCl}_3$ ): 172.03 ( $>\text{C=O}$ ), 165.05 ( $>\text{C=O}$ ), 160.07 ( $-\text{CH}=\text{N}-$ ), 156.8, 153.7, 149.28, 137.1, 133.4, 131.6, 130.4, 127.2, 126.8, 122.3, 121.6, 120.9 (12 C aromatic), 70.32, 69.61, 68.03, 67.05 (4 C,  $\text{C}_5\text{H}_4$ ,  $\text{C}_5\text{H}_5$ ), 34.5–14.2 (17 C aliphatic).  $m/z$ : 766 [M-1].

### Methods

Confirmation of the structures of the products was obtained by  $^1\text{H-NMR}$  and  $^{13}\text{C-NMR}$  spectroscopy, using a Jeol ECA 600 MHz spectrometer with tetramethylsilane as internal standard. IR spectra were recorded using a Nicolet Magna 550 FT-IR spectrometer (NaCl crystal window). Mass spectra were recorded on a Jeol JMS-AX 505 mass spectrometer using the FAB $^+$  method for ionization.

Thermogravimetric experiments were recorded on Paulik–Paulik–Erdéy type Derivatograph MOM Hungary in the following conditions: samples  $m_w=35\pm 5$  mg,  $\text{Al}_2\text{O}_3$  as reference material, heating rate  $10^\circ\text{C min}^{-1}$ , stating conditions, temperature range  $10$ – $900^\circ\text{C}$ .

The processing of the thermogravimetric data was performed using the integrable methods Coats–Redfern [13] and Reich–Lewi [14].

### Results and discussion

The performed reactions are presented in Scheme 2. Table 1 contains the structure of the investigated products.

**Table 1** Structure of compounds

Sample	Z	R
S <sub>1</sub>	$-\text{C}_6\text{H}_4-$	$-\text{C}_{18}\text{H}_{37}$
S <sub>2</sub>	$-\text{C}_6\text{H}_4-$	$-\text{OC}-\text{C}_{17}\text{H}_{35}$
S <sub>3</sub>	$-\text{C}_6\text{H}_4-\text{COO}-\text{C}_6\text{H}_4-$	$-\text{C}_{18}\text{H}_{37}$
S <sub>4</sub>	$-\text{C}_6\text{H}_4-\text{COO}-\text{C}_6\text{H}_4-$	$-\text{OC}-\text{C}_{17}\text{H}_{35}$
S <sub>5</sub>	$-\text{C}_6\text{H}_4-\text{OCO}-\text{C}_6\text{H}_4-$	$-\text{C}_{18}\text{H}_{37}$
S <sub>6</sub>	$-\text{C}_6\text{H}_4-\text{OCO}-\text{C}_6\text{H}_4-$	$-\text{OC}-\text{C}_{17}\text{H}_{35}$

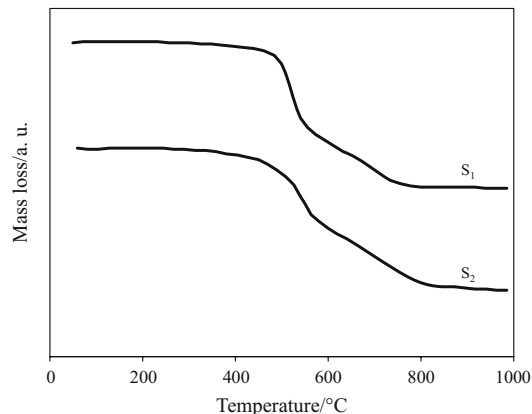
The obtained curves for the S<sub>1</sub> and S<sub>2</sub> samples are presented in Figs 1–3 and in Figs 4–6 for compounds S<sub>3</sub>, S<sub>4</sub>, S<sub>5</sub>, S<sub>6</sub>.

The curves revealed that the initial temperature at which the thermal degradation for the first stage begins is more than  $400^\circ\text{C}$ , which proves a better thermal stability for the analyzed Schiff bases.

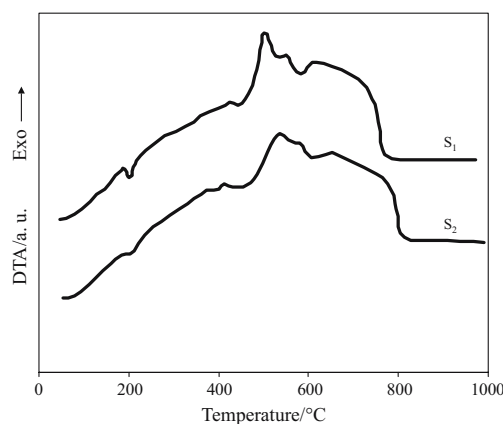
For all samples, the degradation took place in two stages, with different mass loss (Table 2).

Table 2 reveals the TG data such as:  $T_d$  – the onset temperatures,  $T_{\max}$  – temperature of maximum degree rate, mass loss ( $m$ , %) corresponding for each stage and DTA characteristics.

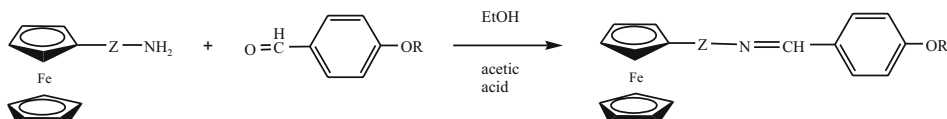
The most important mass loss for S<sub>1</sub>, S<sub>3</sub>, S<sub>4</sub>, S<sub>5</sub>, S<sub>6</sub> has been recorded in the first stage of the thermal degradation, at temperatures onset over  $400^\circ\text{C}$ . In contrast, S<sub>2</sub> have a special behavior, the most important mass loss being recorded in the second stage of the thermal degradation, at temperatures onset be-



**Fig. 1** TG curves for samples S<sub>1</sub> and S<sub>2</sub>



**Fig. 2** DTA curves for samples S<sub>1</sub> and S<sub>2</sub>



**Scheme 2** Synthesis of Schiff bases

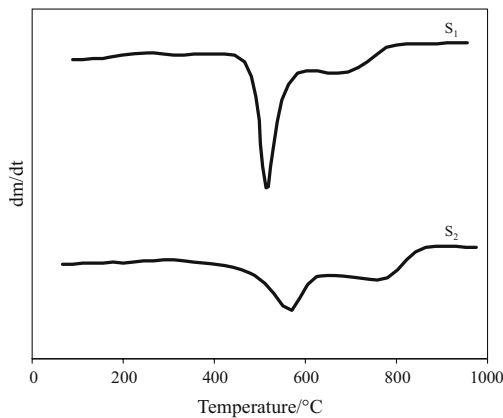


**Fig. 3** DTG curves for samples S<sub>1</sub> and S<sub>2</sub>

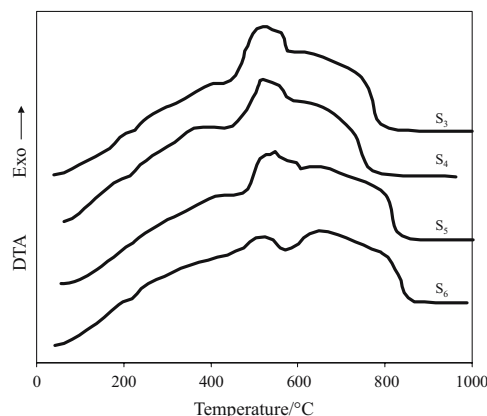


**Fig. 5** DTA curves for samples S<sub>3</sub>, S<sub>4</sub>, S<sub>5</sub> and S<sub>6</sub>

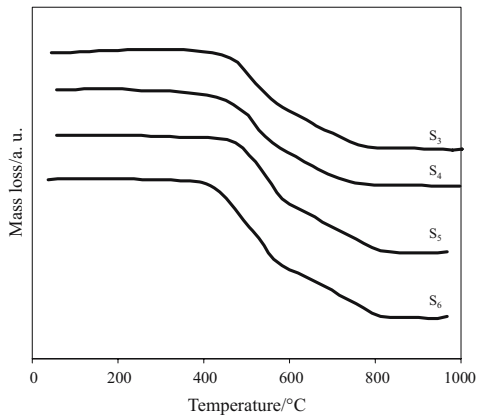
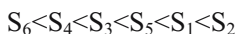


**Fig. 4** TG curves for samples S<sub>3</sub>, S<sub>4</sub>, S<sub>5</sub> and S<sub>6</sub>

tween 580 and 805°C. For all the samples, the degradation processes are not complete, for each case a residue being left.

Using as thermal stability criteria the onset temperatures ( $T_d$ ) for the first stage, the thermal stability series was established as being the following:



The same conclusions regarding the thermal stability are obtained even if is considered the temperature of degradation at maximum degree rate ( $T_{max}$ ) as criteria of stability.

In order to obtain information regarding the degradation mechanism, a kinetic processing of the data, by using the Coats–Redfern integral method, has been made [4]. The obtained results: reaction order ( $n$ ), activation energy ( $E_a$ ), pre-exponential factor ( $\ln A$ ), compensation parameter ( $S_p = E_a / \ln A$ ) and correlation coefficients ( $r^2$ ) are presented in Table 3.

For all the thermal degradation stages the found reaction order was 1. The activation energy for S<sub>2</sub> sample from first stage is bigger than those corresponding to the other sample, fact that demonstrate the higher thermostability, which correspond with the thermogravimetric data from Table 2. By comparing

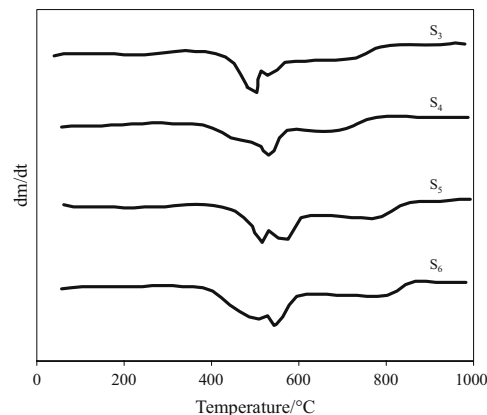
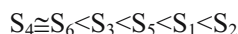


**Fig. 6** DTG curves for samples S<sub>3</sub>, S<sub>4</sub>, S<sub>5</sub> and S<sub>6</sub>

the values of activation energy for the first stage of thermal degradation, the following series of thermal stability of some ferrocene derivatives are obtained. The observed results are in agreement with thermal stability series obtained previously by considering  $T_d$  or  $T_{max}$  as thermal stability criteria.



For getting supplementary evidences regarding the degradation mechanism of the analyzed compounds, a study of the compensation effect has been effectuated. Accordingly, a graphical representation of  $\ln A$  as function of  $E_a$  has been carried out, the compensation equations being represented in Fig. 7.

The linear dependence confirms the similar degradation mechanism of the analyzed compounds in the first stages, the slope of the lines being around 0.15.

In order to obtain supplementary information about the degradation mechanism, the influence of the conversion degree on the activation energy value was evaluated by Reich–Lewi methods. The calculated Reich–Lewi diagrams for analyzed ferrocene derivatives are presented in Figs 8 and 9. The values of the activation energy are grouped according to the two main

**Table 2** Thermogravimetric data

Sample	Stage of thermal degradation	DTA characteristic data	$T_d/^\circ\text{C}$	$T_{\max}/^\circ\text{C}$	Mass loss/%
$S_1$	I	exo	492	519	52.79
	II	exo	552	671	37.14
	residue				10.07
$S_2$	I	exo	505	567	46.24
	II	exo	580	758	48.33
	residue				5.43
$S_3$	I	exo	472	503	48.42
	II	exo	568	661	34.12
	residue				17.46
$S_4$	I	exo	470	490	56.18
	II	exo	550	643	37.46
	residue				6.36
$S_5$	I	exo	484	517	51.30
	II	exo	585	744	31.15
	residue				17.55
$S_6$	I	exo	409	486	50.85
	II	exo	575	733	29.91
	residue				19.24

**Table 3** Kinetic characteristics in non-isotherm conditions

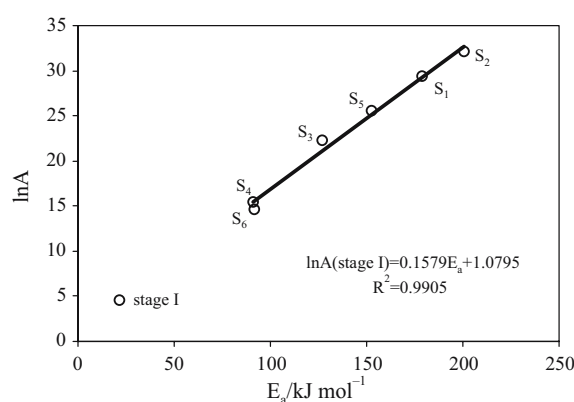
Sample	$n$	$E_a/\text{kJ mol}^{-1}$	$\ln A$	$S_p$	$r^2$
Stage I					
$S_1$	1	178.84	29.34	6.09	0.999
$S_2$	1	200.33	32.14	6.23	0.999
$S_3$	1	126.98	22.22	5.71	0.999
$S_4$	1	91.29	15.49	5.89	0.996
$S_5$	1	152.60	25.55	5.97	0.998
$S_6$	1	91.38	14.62	6.22	0.998
Stage II					
$S_1$	1	98.24	13.60	7.22	0.998
$S_2$	1	101.92	12.50	8.15	0.999
$S_3$	1	112.21	15.41	7.28	0.997
$S_4$	1	100.46	13.93	7.21	0.996
$S_5$	1	90.60	11.58	7.82	0.999
$S_6$	1	95.00	11.76	8.07	0.999

degradation steps. In addition, similar values at conversion values higher than 0.7 were observed.

The results for activation energy obtained by using the Reich–Levi method and the temperature corresponded to the 50% transformation degree are presented in Table 4. By analyzing the calculated values, an agreement with the thermal stability series obtained previously was observed.

**Table 4** Characteristic temperatures and apparent activation energies obtained by the Reich–Levi method at conversion degree  $\alpha=0.5$ 

Sample	$T_{0.5}$ at 50% conversion	$E_a$ at 50% conversion/ $\text{kJ mol}^{-1}$
$S_1$	568	109
$S_2$	607	148
$S_3$	560	100
$S_4$	548	95
$S_5$	577	107
$S_6$	551	87

**Fig. 7** The pre-exponential factor dependence as function of the activation energy

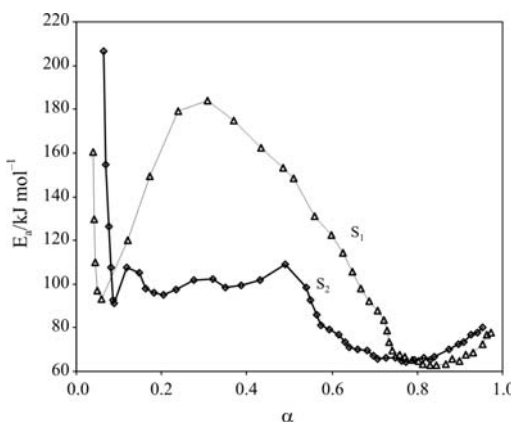


**Fig. 8** Reich–Levi diagrams for sample  $S_1$  and  $S_2$

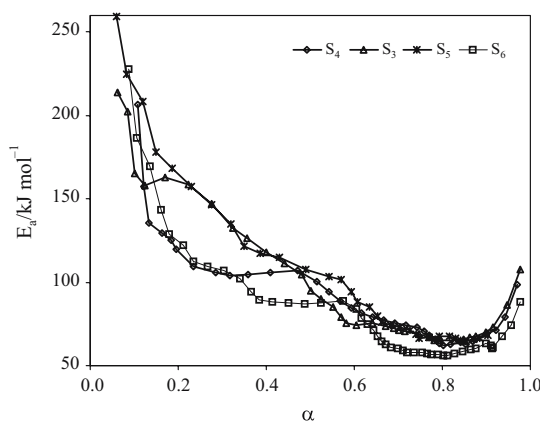


**Fig. 9** Reich–Levi diagrams for sample  $S_3$ ,  $S_4$ ,  $S_5$  and  $S_6$

## Conclusions

The thermal stability and degradation kinetics of ferrocene containing Schiff bases have been reported in this research. Kinetic parameters of degradation were evaluated by using the Coats–Redfern and Reich–Levi methods. The thermal stability series of Schiff bases was established analysis associated with three parameters ( $T_d$ ,  $T_{max}$ ,  $E_a$ ) is:  $S_6 < S_4 < S_3 < S_5 < S_1 < S_2$ .

## Acknowledgements

D. S., G. L. and I. C. gratefully acknowledges for financial support from Ministry of Education of Romania (grant 33371/2004, code CNCSIS 554/40).

## References

- 1 D. Apreutesei, G. Lisa, N. Hurduc and D. Scutaru, *C. E. J. C.*, 2 (2004) 553.
- 2 N. Hurduc, N. Dragoi, C. Ghirvu and N. Hurduc, *J. Therm. Anal. Cal.*, 58 (1999) 525.
- 3 A. Creanga, G. Pokol, N. Hurduc, Cs. Novák, S. Alazaroaie and N. Hurduc, *J. Therm. Anal. Cal.*, 66 (2001) 859.
- 4 N. Hurduc, A. Creanga, Gy. Pokol, Cs. Novák, D. Scutaru, S. Alazaroaie and N. Hurduc, *J. Therm. Anal. Cal.*, 70 (2002) 877.
- 5 K. Shiraishi and K. Sugiyama, *Chem. Express*, 5 (1990) 625.
- 6 N. Shopova and T. Milkova, *Thermochim. Acta*, 356 (2000) 101.
- 7 N. E. A. El-Gamel and G. G. Mohamed, *J. Therm. Anal. Cal.*, 81 (2005) 111.
- 8 N. Foca, G. Lisa and I. Rusu, *J. Therm. Anal. Cal.*, 78 (2004) 239.
- 9 D. Apreutesei, G. Lisa, N. Hurduc and D. Scutaru, *J. Therm. Anal. Cal.*, 83 (2006) 335.
- 10 D. Apreutesei, G. Lisa, D. Scutaru, N. Hurduc, *J. Optoelectronics Adv. Mater.*, 8 (2006) 737.
- 11 A. Togni, T. Hayashi, Eds, *Ferrocenes*, VCH, Weinheim 1995.
- 12 I. Carlescu, N. Hurduc, D. Scutaru, O. Catanescu and L.-C. Chien, *Mol. Cryst. Liq. Cryst.*, 439 (2005) 107.
- 13 A. W. Coats and J. P. Redfern, *Nature*, 201 (1964) 68.
- 14 L. Reich and D. W. Lewi, *Macromol. Chem.*, 66 (1963) 102.

Received: February 8, 2007

Accepted: April 18, 2007

OnlineFirst: June 28, 2007

DOI: 10.1007/s10973-007-8450-8